Engineering Science and Technology, an International Journal 18 (2015) 524–535

HOSTED BY

Contents lists available at ScienceDirect

Engineering Science and Technology, an International Journal

journal homepage: http://www.elsevier.com/locate/jestch

Full length article

Effect of dielectric fluid with surfactant and graphite powder on Electrical Discharge Machining of titanium alloy using Taguchi method

Murahari Kolli*, Adepu Kumar

Department of Mechanical Engineering, National Institute of Technology Warangal, Telangana, India

ARTICLE INFO

Article history:
Received 27 August 2014
Received in revised form
14 January 2015
Accepted 9 March 2015
Available online 16 May 2015

Keywords:
Ti-6Al-4V alloy
Surfactant and graphite powder
Taguchi technique
Material removal rate (MRR)
Recast layer thickness (RLT)

ABSTRACT

In this paper, Taguchi method was employed to optimize the surfactant and graphite powder concentration in dielectric fluid for the machining of Ti-6Al-4V using Electrical Discharge Machining (EDM). The process parameters such as discharge current, surfactant concentration and powder concentration were changed to explore their effects on Material Removal Rate (MRR), Surface Roughness (SR), Tool wear rate (TWR) and Recast Layer Thickness (RLT). Detailed analysis of structural features of machined surface was carried out using Scanning Electron Microscope (SEM) to observe the influence of surfactant and graphite powder on the machining process. It was observed from the experimental results that the graphite powder and surfactant added dielectric fluid significantly improved the MRR, reduces the SR, TWR and RLT at various conditions. Analysis of Variance (ANOVA) and F-test of experimental data values related to the important process parameters of EDM revealed that discharge current and surfactant concentration has more percentage of contribution on the MRR and TWR whereas the SR, and RLT were found to be affected greatly by the discharge current and graphite powder concentration.

1. Introduction

Titanium alloy is increasingly used in many industrial and commercial applications because of its excellent properties. Titanium alloy finds enormous applications in chemical industry, machine building, shipbuilding and auto industry apart from the fabrication of equipment for the oil and gas industry, food industry, medicine and civil engineering. The largest consumer of titanium alloys is the aerospace industry For example, 14 percent of the total airframe of Boeing 787 is made of Ti alloy [1,2]. Ti-6Al-4V is being extensively used in engineering applications owing to its outstanding corrosion resistance, fatigue resistance and in many environments especially in high strength applications.

Ti-6Al-4V is $\alpha+\beta$ alloys which contain a large amount of β stabilizers (4–6 %). Beta alloys can be heat treated to develop a variety of microstructures and mechanical property combinations. Titanium alloy of VT6 grade has the following chemical composition (wt. %): Al, 5.5–7.0; V, 4.2–6.0. The content of impurities should not exceed (wt. %): C, 0.10; Fe, 0.30; Si, 0.15; O2, 0.20; N2, 0.05; H2, 0.015 [3]. Titanium alloy has high strength to weight ratio, high temperature strength and it is difficult to machine titanium with the conventional machining process due to its chemical reactivity with almost all cutting tool materials, and its low thermal conductivity and low modulus of elasticity impairs machinability [4,5]. Dornfeld et al. [6] investigated poor machining characteristics on titanium alloys using conventional machining. Non conventional thermo-electric spark erosion machining process, commonly known as electric discharge machining (EDM) has been successfully used to machine titanium and its alloys effectively regardless of their chemical and mechanical properties. In EDM, electrode and work piece do not come in contact with each other for the machining of the material and the material removal mechanism uses the electrical energy which is converted into thermal energy through a series of discrete electrical discharge energy obtained between the cathode (work piece) and the anode (electrode) sinking in an insulating dielectric fluid.

Therefore, hard metals like Titanium, Nickel, ceramics and ferrous alloys can be machined effectively using EDM. For the EDM machining, selection of proper process parameters is important. An improper combination of process parameters may result in lower

* Corresponding author. Tel.: +91 9985668751; fax: +91 08702462834.
E-mail address: kmhari.nitw@gmail.com (M. Kolli).
Peer review under responsibility of Karabuk University.

http://dx.doi.org/10.1016/j.jestch.2015.03.009

MRR, increased SR, high tool wear rate (TWR), higher RLT that impose higher machining cost. Optimization of EDM process parameters by finding the correct combination of the process parameters available in EDM will enhance the machining productivity and reliability.

Further, for improving the machining efficiency, material removal rate and surface roughness with reduced recast layer thickness of titanium alloy using EDM, many researchers have attempted different techniques such as Ultrasonic Vibration Assisted EDM (UVAEDM) [7], Rotary Assisted EDM (RAEDM) [8], Magnetic Assisted EDM (MAEDM) [9], and Ultrasonic with Rotary Assisted EDM (URAEDM) [10], Gas Assisted EDM (GAEDM) [11], Cryogenic Assisted EDM (CAEDM) [12] and Powder Mixed EDM (PMEDM) [13,14], However, it has been found that there are few reports on powder added to dielectric fluid on EDM, and there is a very limited work available on surfactant and graphite powder mixed EDM of Titanium alloy [15,16].

For instance, Takashi et al. [7] found that the ultrasonic vibrating movement of the work piece improves the slurry circulation and the high frequency pumping action, by pushing the debries away and sucking the new fresh dielectric, stoutly ameliorates the discharge energization, increases their efficiency and gives a higher MRR and lower TWR. UV plays dual role in EDM such as a direct contribution to material removal and facilitating better machining conditions for surface finish by EDM. Chow et al. [8] examined the micro-slit operation on Ti-6Al-4V with modified rotary disc copper electrode and addition of Al and SiC powders separately in kerosene as dielectric in EDM process. The negative polarity was employed. It has been observed that the gap between the electrode and the work piece is increased slightly due to the addition of powders. This increases MRR and disperses several discharges in several increments due to which particle size of debris is reduced so that they are removed easily with increase in SR. MRR is more when SiC is added to kerosene than aluminum. Govindan et al. [11] investigated on dry EDM using helium gas dielectric; they observed that lower MRR and TWR were obtained. Similarly, SEM micrographs of dry EDMed surfaces using helium gas dielectric showed a few micro cracks and had a glowing appearance, which indicates that the quality of surfaces generated using helium is better as compared to oxygen.

Abdulkareem et al. [12] studied the effect of cryogenic cooling on TWR of copper electrode and SR during EDM of Ti-6Al-4V. It has been investigated that the liquid nitrogen reduces the temperature of copper electrode, thus decreasing its melting and vaporization. It also improves electrical and thermal conductivities of copper. They also observed that TWR and SR reduces due to the efficient heat transfer away from the electrode. Jeswani et al. [13] studied the effect of addition of graphite powder to kerosene used as the dielectric fluid during the EDM. It is observed that adding graphite powder to kerosene changed the ionization-deionization characteristics of the liquid to permit more spark discharges per unit time. The reduction in the breakdown voltage results in a higher discharge frequency which in turn increases the MRR. Kibria et al. [14] compared the effect of various dielectrics such as kerosene, de-ionized water and mixing of B_4C powder in the kerosene and de-ionized water during micro-hole machining of Ti-6Al-4V using EDM. It has been noticed that MRR and TWR are more using de-ionized water than kerosene. When B_4C powder mixed dielectrics are used, MRR increases with de-ionized water, but TWR decreases with kerosene. It has been also observed that the RLT is less in case of de-ionized water as compared to kerosene.

The additives like graphite powder and surfactant are added into the dielectric fluid for better circulation in the discharge gap and to avoid the particle agglomeration. During the machining process, particles that enter into the discharge gap breakdown the voltage easily which reduces the insulating strength by increasing the discharge gap and passage and also discharge evenly distributed entire the machining process. As a result, the process becomes more stable; thereby improving the machining efficiency, which lowers the surface roughness, recast layer thickness and increases the material removal rate.

Till date, researchers have attempted various surfactant and powders added into dielectric fluid of different materials. For instance, Murahari and Kumar [15,16] investigated the effect of additives added in dielectric fluid on EDM of Titanium alloy. The concentration of surfactant and discharge current were varied keeping other parameters as constant to measure the effect on MRR, SR and TWR. It was concluded that with increasing surfactant concentration and discharge current, MRR increases. Kun Lin Wu et al. [17] carried out an experimental investigation of surfactant mixed with EDM for SKD 61steel. Parameters such as discharge current, pulse on time, open voltage and gap voltage were changed to explore the results with the addition of surfactant to dielectric fluid, which increases the conductivity and machining efficiency. It was observed that MRR is higher in case of span 20 than span 80. The maximum MRR is obtained with span 20 of concentration 30 (g/lit). The MRR is found to be 40 % higher than that of pure kerosene without affecting the SR much.

Wu et al. [18] investigated the improvement of surface finish on SKD61 steel using EDM with three dielectrics pure kerosene; aluminum powder added kerosene and kerosene with aluminum powder and surfactant added dielectric. It was concluded that insulation is lowered and the gap distance between electrodes is increased with Al powder added dielectric and the surfactant added in dielectric. The thin optimized recast layer can be achieved when the dielectric is mixed with both aluminum powder and surfactant due to well dispersed aluminum powder and uniform distribution of discharge energy during EDM process. A.S. Dukhin and P.J. Goetz [19] conducted the experimental study of non-ionic surfactants and 5 % Alumina AKP 30 added to non-polar liquids (kerosene). span 20 and span 80 surfactants were compared with water and kerosene. It was observed that 5 % alumina and span 20 added to kerosene produced better dispersion effect compared to span 80 and it was also concluded that two mechanisms are involved in this study: dissociation of the span molecules and apparent dissociation constant with HLB.

Zhang et al. [20] presented a new process water in oil emulsion (W/O) mixed with EDM, and considered the machining parameters such as peak current, dielectric and pulse duration and studied their effects on machining performances such as MRR, SR and relative tool wear rate (RTWR). It was observed that increase in the MRR enhanced the relative electrode wear rate (REWR), due to the high viscosity of dielectric fluid which can restrict the expansion of the discharge channel; the impulsive force acts on a mined area. The analysis of MRR results showed that the increase in the discharge current increased the discharge energy and impulse force. Yanzhen Zhang et al. [21] studied different dielectric fluids used in EDM and measured the characteristics of the recast layer and relationships of other machined parameters. It was observed that the recast layer formed in W/O emulsion exhibited larger surface roughness, thickness and micro hardness compared to that formed in kerosene and deionized water.

Konig et al. [22] studied aqueous solutions of organic compounds such as dielectric working media for Die Sink EDM. In this process the dielectric was mixed with glycerine, under the working conditions of discharge current, long pulse duration and high duty factor. It was concluded that tool electrode wear was reduced under the roughing conditions (high discharge current) which improved the machining conditions (MRR). When water is the dielectric fluid,

Table 1
Chemical composition of Ti-6Al-4V alloy.

Element	C	Al	V	N	O	Fe	H	Ti
%	Max. 0.014	6.07	4.02	0.0036	0.1497	0.03	0.0115	Balance

surface roughness is lowered and the metal characteristics of the surface are degraded.

In the present work, L_9 orthogonal array with various sets of experiments at different concentrations of surfactant and graphite powder in the dielectric fluid were carried out to study the effect of these concentrations on the MRR, SR, TWR and RLT with respect to discharge current. Further study was carried out to observe the influence of surfactant, graphite powder and discharge current on the presence of elements on the machined surface using Energy Dispersive X-ray Spectroscopy (EDS) along with the surface topography with the help of scanning electron microscope (SEM).

2. Scheme of experimental procedure

2.1. Selection of tool and work materials

The material used for the experiments was Titanium (Ti-6Al-4V) alloy Grade 5 (Mishra Dhatu Nigam Ltd. Hyderabad). The material samples were rectangular type with dimensions of 100 mm length, 50 mm width and 5 mm thickness. The chemical composition and mechanical properties of Ti-6Al-4V are shown in Tables 1 and 2. Copper was selected as an electrode material with 14 mm diameter and 70 mm length because of its high thermal and electrical conductivity.

2.2. Selection of process parameters

There are a large number of input process parameters to be considered within the EDM process for determining the optimal process parameters. Considering the related studies, it was concluded that process parameters such as discharge current, graphite powder and surfactant concentration have a clear influence on the EDM performance of Titanium alloy [15,16]. Before performing the main EDM tests, pilot experiments were been done. In pilot experiments the range of variations for discharge current were between 5 and 20 A and when the discharge current was kept above 10 Amp, it was observed that MRR was significant and when a current of more than 20 Amp was selected, it resulted in higher MRR necessitating the selection of the values [15,16,23]. The pilot experiments were carried out with the addition of graphite powder ranging from 1 to 20 g/lit into the dielectric fluid to study the effect of MRR and SR. From the results, it is observed that at 14 g/lit graphite powder concentration resulted better in MRR and SR. Hence for further experimentation, the graphite powder concentration is fixed at 14 g/lit. The graphite powder morphology can be

Table 2
Properties of Ti-6Al-4V alloy.

Property	Values
Hardness (HRC)	32–34
Melting point (°C)	1649–1660
Density (g/cm^3)	4.43
Ultimate tensile strength (MPa)	897–950
Thermal conductivity (W/m K)	6.7–6.9
Specific heat (J/kg K)	560
Mean coefficient of thermal expansion (W/kg K)	8.6×10^{-6}
Volume electrical resistivity (ohm-cm)	170
Elastic modulus (GPa)	113–114

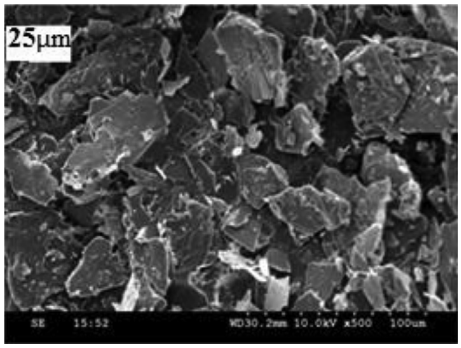

Fig. 1. SEM morphology of graphite powder particles (μm).

observed as shown in Fig. 1. The concentration of the Surfactant was varied between 0.25 g/lit and 15.0 g/lit but the surfactant that showed more than 10 g/lit concentration did not show any considerable improvement in the performance characteristics. The range selected for the pulse on time and pulse off time is based on the pilot experiments and literature. So, in this study these three main EDM parameters were selected as variable input parameters by keeping other process parameters constant. The graphite powder and surfactant properties are presented in Tables 3 and 4 respectively. The working range of the process parameters selected under the present study is presented in Table 5.

2.3. Selecting the L_9 orthogonal array

The numbers of process parameters considered were three, and the level of each parameter was three. The degrees of freedom of all three parameters were two (i.e. number of levels-1) and the total degrees of freedom of all the factor are 6 (i.e. $3 \times 2 = 6$). The selected Orthogonal Arrays (OA) degrees of freedom (DOF) (i.e. number of experiments $- 1 = 9-1 = 8$) must be greater than the total DOF of all the factors (6). Hence, L_9 (3^4) OA is considered for the present study. Based on the preliminary experimentation, there was no interaction between the selected process parameters. Hence, an interaction was not considered for the present study. Three trials of each experiment were conducted and average of these three values was presented to minimize the pure experimental error. The selected OA is presented in Table 6.

2.4. Experiments setup

A series of experiments were conducted on a die sinking FORMATICS EDM machine of type EDM-50 with Electronica PSR-20 controller. Fig. 2 shows a photograph of the equipment and experimental constant parameters are tabulated in Table 6. The EDM machine has a DC servo system. The work piece was firmly clamped in the vice and immersed in the EDM oil. The maximum discharge current is 20 A, power factor is 0.8 and minimum surface finish is 0.8 microns. In this experimental study, spark erosion 450

Table 3
Properties of graphite powder (average size: 20 μm).

Parameter	Symbol	Quantity
Density	g/cm^3	1.90–2.30
Elastic module	Tpa	1
Strength	Gpa	130
Electrical resistivity	μΩ cm^{-1}	3×10^{-3}
Thermal conductivity	W cm^{-1} K^{-1}	1.50
Thermal expansion	K^{-1}	1×10^{-1}
Melting point	K	3652–3697 °C

Table 4
span 20 Surfactant properties.

Property	Quantity
Chemical formula	$C_{18}H_{34}O_6$
Molecular weight	346.47(g/mol)
Density	1.032 g/ml at25 °C (L)
Flash point	>230 °F(110 °C)
Relative index	n 20/D 1.4740 (L)
HLB value	8.6
Water content	<1.5 (%)
Acid value	4–8
Heavy metal (PPM)	9.5–10.0
Saponification Value	158–170

Table 5
Working range of the process parameters and their levels.

Symbol	EDM parameter	Unit	Level 1	Level 2	Level 3
A	Discharge current	A	10	15	20
B	Surfactant concentration	g/lit	4	6	8
C	Graphite powder concentration	g/lit	4.5	9	13.5

EDM oil (obtained from Electronica machine tools limited, Pune, India) was used as dielectric fluid because of its high dielectric strength, high flash point, less surface tension and less density. The experiments were conducted as per L_9 OA selected as shown in Table 7. Each experiment was conducted for thirty minutes. Before machining, the work pieces and electrodes were cleaned with acetone and polished with various emery papers (180–1600 grit sizes). Negative polarity was used during the experiments.

2.5. Performance characteristics calculation

EDM performance characteristics, regardless of the type of the electrode material and dielectric fluid are measured usually by the following criteria:

- Material Removal Rate (MRR) (mm^3/min)
- Surface Roughness (Ra)
- Tool wear rate (TWR) (mm^3/min)
- Recast layer thickness (μm)

The MRR is defined as the work piece weight loss (WWL) under a period of machining time in minutes, i.e.

$$\text{MRR}\quad (\text{mm}^3/\text{min}) = \frac{\text{WWL (g)} \times 1000}{\rho w\ (\text{g/cm}^3)\ \times \text{Tm(min)}}$$

$$\text{WWL}\ (\text{mm}^3/\text{min}) = (W_b - W_a)$$

Table 6
Experimental layout using an L9 (3^4) orthogonal array.

S. no	Process parameters		
	Discharge current (A)	Surfactant concentration (B)	Graphite powder concentration (C)
1	1	1	1
2	1	2	2
3	1	3	3
4	2	1	2
5	2	2	3
6	2	3	1
7	3	1	3
8	3	2	1
9	3	3	2

Fig. 2. Modified experimental setup.

where:

W_b = weight of work piece material before machining (g)
W_a = weight of work piece material after machining (g)
T_m = machining time (min)
ρ_w = density of work piece material (g/cm^3).

Maximum MRR is an important indicator of the efficiency and cost effectiveness of the EDM process. However, high MRR is not always desirable for all applications, since this may scarify the surface integrity of the work piece. A rough surface finish is the outcome of high removal rates.

In terms of the TWR value, the equation below is usually used as; The TWR is the tool weight loss (TWL) under a period of machining time in minutes, i.e.

$$\text{TWR}\ (\text{mm}^3/\text{min}) = \frac{\text{TWL (g)} \times 1000}{\rho t\ (\text{g/cm}^3)\ \times \text{Tm(min)}}$$

$$\text{TWL}\ (\text{mm}^3/\text{min}) = (T_b - T_a)$$

where:

T_b = weight of tool material before machining (g)
T_a = weight of tool material after machining (g)
T_m = machining time (min)
ρ_t = density of tool material (g/cm^3).

The concept of TWR can be defined in different ways, and in this study the TWR is defined according to the weight loss of the electrode, as this definition is the most commonly used among the researchers. The minimum value of TWR always becomes an objective in many studies, where it indicates a minimum change in the shape of electrode, which leads to the better accuracy of the product.

SR is calculated by using surface roughness tester (Handysurf instrument). Surface roughness is the roughness or smoothness of a given surface. In this study, it is measured in terms of R_a (Roughness average), which is an arithmetic average of peaks and valleys of a

Table 7
Experimental settings.

Working parameters	Description
work piece material	Ti-6Al-4V
Size of work piece	100 mm × 50 mm × 5 mm
Electrode material and size	Electrolyte copper
Size of electrode	ϕ 14 mm × 70 mm
Electrode polarity	+ ve (reverse polarity)
Dielectric fluid	Spark erosion 450 EDM oil
Discharge open voltage	110 V
Discharge gap voltage	65 V
Flushing pressure	0.75 MPa
Machining time	30 min

work piece surface measured from the centerline of evaluation length.

After machining, the samples were cut cross-sectionally using wire Cut EDM machine. The cross sectioned samples were mirror polished and suitable etchant (Distilled water, HF and HNO3, 20:1:1) was applied for microstructural observation. While in wire cut-EDM the microstructural area of samples may change, during the sample cutting processes. The embedded samples were abraded for relatively longer time to remove the recast layer and the heat affected zone caused by the wire EDM processes, before mirror polishing. By using image analyzer software it was found that the recast layers of the samples were not uniform. For each sample, at four different locations, the recast layer thickness was measured and then the average value was taken [24]. Fig. 3 shows the SEM micrographs of recast layer. All the SEM images are taken under the same conditions.

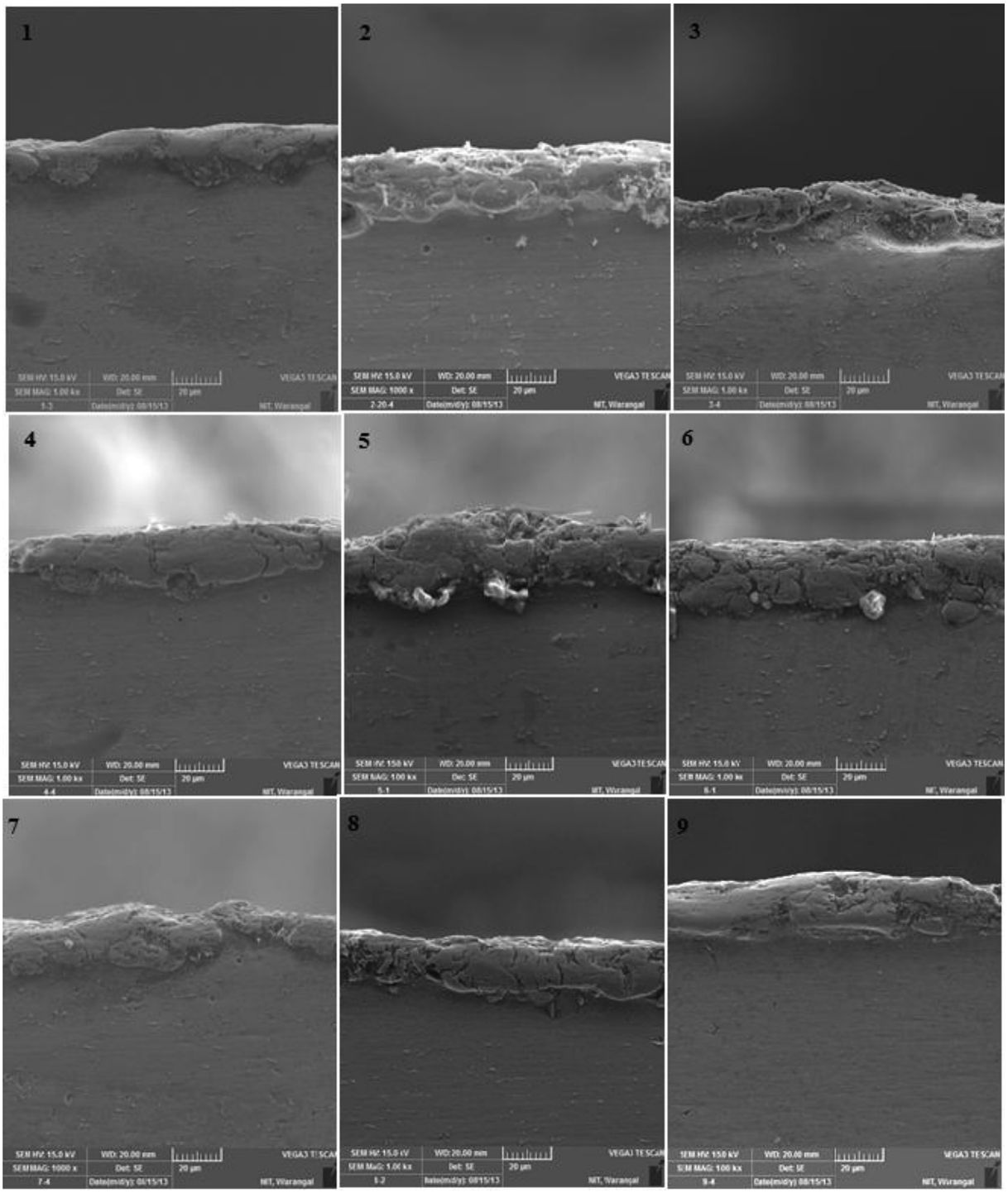

Fig. 3. SEM micro-graphs of EDMed RLT samples.

2.6. Identify the optimum output performance condition and their effect of parameters

Taguchi technique is very efficient to deal with responses affected by many parameters. It is easy, effective and an efficient approach to determine optimal process parameters. It is a powerful design of experiments tool which reduces drastically the number of experiments required to model and optimize the responses. It also saves a lot of time and experimental cost. Taguchi method is devised for process optimization and identification of optimum levels of process parameters for given responses. In Taguchi method, the experimental values of various responses are further transformed from signal to noise (S/N) ratio. The response that is to be maximized is called 'higher the better' and the response that is to be minimized is called 'lower the better' [25–27]. Taguchi uses the S/N ratio to measure the deviation of the response from the mean value. S/N ratios for 'higher the better' and 'lower the better' characteristics are calculated using Equations (1) and (2) respectively,

$$\eta = -10 \log_{10}\left[\frac{1}{n}\sum_{i=1}^{n}\frac{1}{y_i^2}\right] \quad (1)$$

$$\eta = -10 \log_{10}\left[\frac{1}{n}\sum_{i=1}^{n}y_i^2\right] \quad (2)$$

where η denotes the S/N ratio of experimental values, y_i represents the experimental value of the ith experiment and n is the total number of experiments. By using above equations the S/N ratio values of machining performance for each experiment of L_9 orthogonal array can be calculated for the MRR, SR, TWR and RLT and the values are presented in Table 8. By using the experimental results and worked out the values of the S/N ratios, average effect response value and the average S/N response ratios are calculated for MRR, SR, TWR and RLT and are presented in Table 9. The S/N ratios, response graphs for MRR, SR, TWR and RLT are shown in Figs. 4–7 respectively. A higher S/N ratio values corresponds to a better performance. Hence the parameters for the highest S/N ratio values will be the optimum level parameters.

3. Results and discussion

3.1. Material removal rate

Table 9 shows the orthogonal array based experimental results of MRR and its corresponding signal to noise ratio (S/N), whose analysis of variance (ANOVA) results are listed in Table 10. The ANOVA results and F-test values indicate that the most significant factor is discharge current (81.83 %) compared to other factors like surfactant concentration (5.97 %) and graphite concentration (10.53 %). The main S/N ratio response graph shown in Fig. 4(A) infers that MRR increases with an increase in discharge current. As the discharge current is higher, the discharge energy is also higher. Hence, the higher discharge energy distributed into high melting temperature, it causes high evaporation and high impulsive force acting on machining region related to higher MRR [28]. In other words, higher discharge current is the key factor to obtain the higher material removal rate in EDM of Titanium alloy.

The effect of span 20 surfactant concentration on the MRR is illustrated in Fig. 4(B). The material removal rate initially increases with increasing surfactant concentration and then decreases with further increase in surfactant concentration. It is known that increasing the surfactant concentration increases the conductivity of dielectric fluid, the surface tension, dispersion and dissolubility of particles which increases the MRR [19]. Increasing Hydrophilic Lipophilic Balance (HLB) value replicates more polarity of the surfactant and due to this span 20 surfactant is added in the EDM oil (non-polar group) while the hydrophilic head group absorbs the surface of graphite particles and the hydrophobic tail extends to the dielectric fluid. The agglomerated graphite particles are to be retarded because the stereo-barriers exited or were involved [18]. Surfactant concentration effect well distributions of graphite powder in the dielectric are accomplished. Concentration of the surfactant increases the viscosity of the dielectric fluid because of which the eroded material finds it difficult to exist in the machined zone. The decrease in MRR is due to the effect of powder particles, vanderwaal forces, electrostatic forces, particle size, magnification and surface properties [29]. This type of organic components has large molecular structure and is easily decomposed in the dielectric fluid to produce more gases and carbon dregs, which affect the machining zone [30].

The influence of graphite powder concentration on MRR is shown in Fig. 4(C). This figure indicates that the value of MRR increases with an increase in graphite powder concentration. When powder is added to dielectric fluid, the powder particles get energized and behave in a zigzag manner when the voltage is applied across the electrodes. They form a chain like structure in the spark gap. This chain helps in bridging the gap between the work piece and the electrode. This also reduces the gap voltage and dielectric strength of dielectric fluid and this initiates series discharge. The sparking frequency is increased with improved flushing of debris effectively away from the gap. This results in effective discharge transmissivity under the sparking area due to increase in the thermal conductivity. Hence, MRR increases in powder mixed dielectric fluid [18,31].

Fig. 4 shows the $A_3B_2C_3$ parameters, i.e. discharge current of 20 Amp, surfactant concentration of 6 g/lit and graphite powder concentration of 13.5 g/lit respectively are the optimal conditions for better MRR. Further the empirical model has been developed to predict the MRR values using regression analysis, including up to the square terms in the model. The regression equation is

Table 8
Average results of MRR, SR, TWR and RLT.

Ex no.	Discharge current (A)	Surfactant concentration (g/lit)	Graphite concentration (g/lit)	[a]MRR (mm^3/min)	[a]SR (Ra) (μm)	[a]TWR (mm^3/min)	[a]RLT (μm)
1	10	4	4.5	2.8045	1.9	0.85	13.26
2	10	6	9	3.9630	2.4	0.66	21.78
3	10	8	13.5	3.6057	3.0	0.35	16.98
4	15	4	9	5.2503	2.8	1.35	20.39
5	15	6	13.5	5.5625	3.2	1.2	22.97
6	15	8	4.5	4.4736	3.8	1.53	21.83
7	20	4	13.5	5.9367	3.4	1.9	20.84
8	20	6	4.5	5.5180	3.7	2.3	23.66
9	20	8	9	5.1923	4.2	2.15	23.78

[a] Average valves.

Table 9
Average results of MRR, SR, TWR and RLT their corresponding S/N ratios.

Sl. no	MRR (mm^3/min)	S/N ratio (dB)	SR (Ra) (μm)	S/N ratio (dB)	TWR (mm^3/min)	S/N ratio (dB)	RLT (μm)	S/N ratio (dB)
1	2.8045	8.9571	1.9	−5.58	0.85	1.41	13.26	−22.45
2	3.9630	11.9605	2.4	−7.60	0.66	3.61	21.78	−26.76
3	3.6057	11.1398	3.0	−9.54	0.35	9.12	16.98	−24.60
4	5.2503	14.4037	2.8	−8.94	1.35	−2.61	20.39	−26.19
5	5.5625	14.9054	3.2	−10.10	1.20	−1.58	22.97	−27.22
6	4.4736	13.0131	3.8	−11.59	1.53	−3.70	21.83	−26.78
7	5.9367	15.4709	3.4	−10.62	1.90	−5.57	20.84	−26.37
8	5.5180	14.8356	3.7	−11.36	2.30	−7.23	23.66	−27.48
9	5.1923	14.3072	4.2	−12.46	2.15	−6.64	23.78	−27.52

$MRR = -6.30 + 0.826A + 1.12B + 0.146C - 0.0210A * A - 0.101B * B - 0.00420C * C$, R-Sq = 99.5 %, R^2 and R^2 adj values of the model are in the acceptable range of variability in predicting MRR values.

3.2. Surface roughness

Table 9 shows the orthogonal array based experimental results of SR and its corresponding signal to noise ratio (S/N), whose analysis of variance (ANOVA) results are listed in Table 11. The ANOVA results and F-test values show that the most important parameters are discharge current (65.00 %) and surfactant concentration (34.00 %). Fig. 5(A) represents the relationship between the discharge current and surface roughness. The experimental results reveal that the pulse on time and pulse off time constant condition the surface roughness trend (is not good to) increase gradually as it increases the discharge current. The surface roughness is associated with discharge current which affects the melting, evaporation and exhaust removal of material. Lower discharge current results in lower energies. Lower discharge energies are responsible for less impulse forces, on the discharge zone and for the formation of small craters and small cavities on the machined surface resulting in high surface finish [32]. High discharge current produces high discharge energy, can be reached in a plasma channel may expand with more melting materials formed on discharge gap. Then the high impulsive forces are formed deeper and larger craters on the machined surface and more melted material will be removed which obtain rough surface. The discharge current increases and the surface roughness increases, which increases the machining efficiency [33].

Fig. 5(B) shows the variation of surface roughness with span 20 Surfactant concentrations added in a dielectric fluid. It is observed that the increase in the concentration of span 20 surfactant increases the surface roughness, which eliminates the aggregation of particles. The surfactant when added plays a different role in the dielectric fluid. These included wetting the powder, displacing the trapped air and disaggregation or fragmentation of the particle clusters which prevent reaggregation of the dispersed particle [34,35]. Due to this the surface roughness increases with increase in the concentration.

Fig. 5(C) represents the relationship between the concentration of graphite powder and surface roughness. Graphite powder added into dielectric fluid easily collapses the insulation, which reduces the electrical resistivity of the fluid and increases the discharge gap and results in reducing the impulse force of the discharge channel [18]. This effect on machining gap produces a high plasma channel (high heat transfer) from work piece to the tool which increases the material removal rate [36]. The machined surface shows uneven sizes of debris and craters which results in reduction of surface finish. After that dielectric fluid segment, graphite powder concentration is increased and the machining gap is reduced. Hence, it drastically increases the conductivity and impulsive forces, resulting in high electrical discharge energy density and high gas explosion. When gas explosion starts melting and evaporation take place and the plasma zone is extended. The later machined surface has large, deeper craters which increases the surface roughness.

Fig. 5 shows the $A_1B_1C_1$ parameters, i.e. discharge current of 10 Amp, surfactant concentration of 4 g/lit and graphite powder concentration of 4.5 g/lit respectively are the optimal conditions for SR. Further the empirical model has been developed to predict the SR values using regression analysis, including up to the square terms in the model. The regression equation is $SR = -0.944 + 0.333A - 0.008B - 0.0222C - 0.00667A * A + 0.0208B * B + 0.00165C * C$, R-Sq = 99.6 %, R^2 and R^2 adj values of the model are in the acceptable range of variability in predicting SR values.

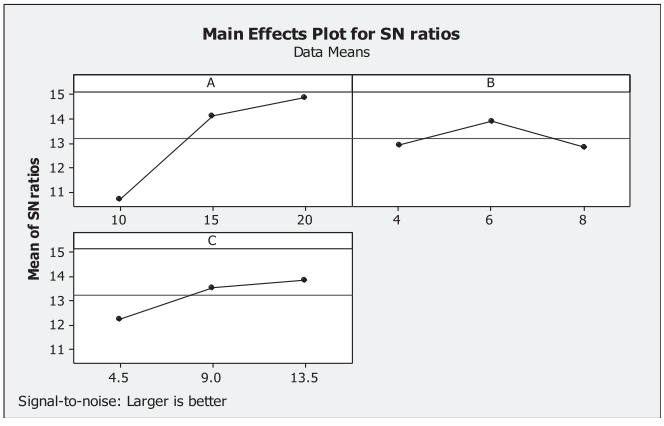

Fig. 4. S/N response graph for material removal rate.

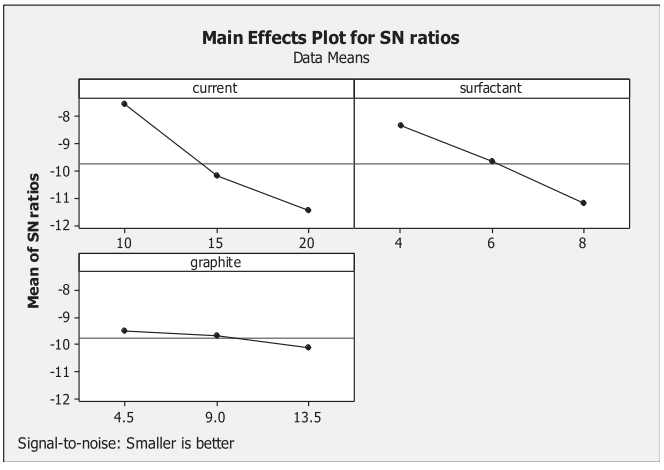

Fig. 5. S/N response graph for surface roughness.

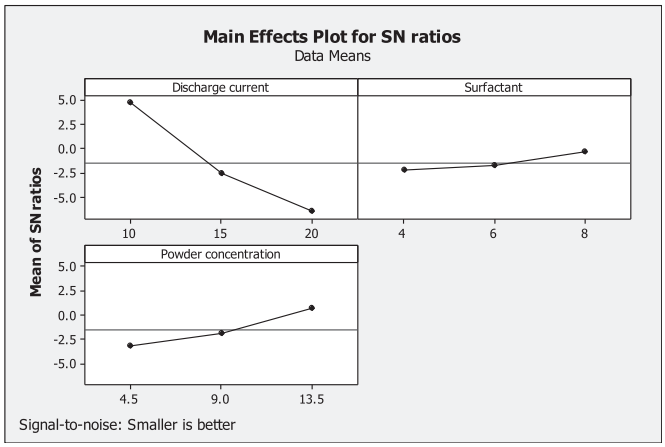

Fig. 6. S/N response graph for tool wear rate.

3.3. Electrode wear rate

The experimental values and its S/N ratios of TWR are shown in Table 9. According to the orthogonal array based experiments, the higher S/N ratio of the response graph shows better performance of the process. The corresponding ANOVA results and F-test values are listed in Table 12 and also the process parameters are significant at 95 % confidence level. Fig. 6(A) reveals that with increasing discharge current the TWR increases. When discharge current increases the pulse energy also increases and thus high heat energy is produced in the work piece–electrode interface that leads to increased melting and evaporation of the tool resulting in increased TWR. From Fig. 6(B), it is evident that an increase in the surfactant concentration decreases the TWR. For the reason that; as a result of surfactant added in the dielectric fluid reduces the TWR linearly. Intense movement of electrons because of small arcs produced during the machining may reverse the direction of the feed to maintain a larger gap and as a consequence, most of the (−ve) ions move easily through the machining gap and results in lower TWR [37].

Fig. 6(C) represents the relationship between the graphite powder and tool wear rate. It revealed that the TWR reduced with increasing the graphite powder concentration. Due to the fact that graphite powder addition in to EDM oil disturbs the adherence of nuclides attached to the surface of the electrode and reduces the TWR. Due to the presence of graphite particles equal distribution of discharge energy and better conduction of discharge intensity results in nominal TWR. A similar result has been reported by Kansal et al. and Kibria et al. [14,31] they found that the powder properties (i.e. concentration, size, density, electrical resistivity and thermal conductivity) are significantly affected the machining performance of appropriate amount of powder to the dielectric fluid reducing the TWR.

Fig. 6 shows the $A_1B_3C_3$ parameters, i.e. discharge current of 10 A, surfactant concentration of 8 g/lit and graphite powder concentration of 13.5 g/lit respectively are the optimal conditions for TWR. Further the empirical model has been developed to predict the TWR values using regression analysis, including up to the square terms in the model. The regression equation is $TWR = -0.743 + 0.140A + 0.092\ B - 0.019C + 0.0002A * A - 0.008\ B * B - 0.001C * C$, R-Seq = 99.8, R^2 and R^2 adj values of the model are in the acceptable range of variability in predicting TWR values.

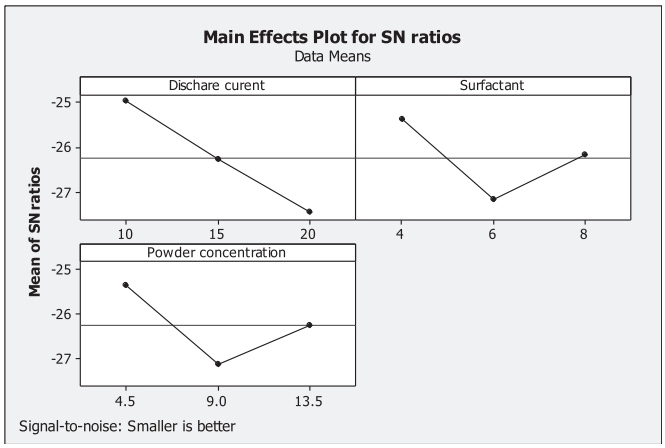

Fig. 7. S/N response graph for recast layer thickness.

3.4. Recast layer thickness

Table 9 shows the orthogonal array based experimental results of RLT and its corresponding signal to noise ratio (S/N), whose analysis of variance (ANOVA) results are listed in Table 13. The ANOVA results and F-test values indicate that the most significant factors are discharge current (50.88 %) and surfactant concentration (32.32 %). The S/N response graph in Fig. 7 shows that the RLT decreases upon decreasing the discharge current and surfactant concentration. In other words, graphite powder concentration (11.03 %) is a less significant factor to obtain the lower recast layer thickness in EDM of Titanium alloy.

Fig. 7(A) represents the relationship between the discharge current and recast layer thickness. The experimental results revealed that increase in the discharge current increases the recast layer thickness, due to Titanium material properties are different compared to steel and other materials. Titanium has high electrical resistivity and low thermal conductivity and its machining

Table 10
ANOVA analysis for MRR.

Source	DF	SS	MS	F	P	% Contribution
A	2	7.26	3.63	49.27	0.020	81.83
B	2	0.53	0.26	3.59	0.218	05.97
C	2	0.93	0.47	6.34	0.136	10.53
Error	2	0.15	0.07			01.67
Total	8					100

Table 11
ANOVA analysis for SR.

Source	DF	SS	MS	F	P	% Contribution
A	2	2.62	1.36	175.00	0.006	65.00
B	2	1.41	0.70	91.00	0.011	34.00
C	2	0.13	0.03	0.057	0.638	0.70
Error	2	0.04	0.00			0.30
Total	8					100

Table 12
ANOVA analysis for TWR.

Source	DF	SS	MS	F	P	% Contribution
A	2	174.20	87.10	34.84	0.002	75.74
B	2	20.45	10.23	4.09	0.043	08.71
C	2	30.73	15.36	6.14	0.026	13.39
Error	2	4.99	2.50			02.16
Total	8					100

Table 13
ANOVA analysis for RLT.

Source	DF	SS	MS	F	P	% Contribution
A	2	49.70	24.86	13.79	0.068	50.88
B	2	32.58	16.29	9.04	0.100	32.32
C	2	9.18	4.59	2.55	0.282	11.03
Error	2	3.60	1.80			05.77
Total	8					100

discharge current is applied to machined zone, so that the material temperature and electrical resistivity is increased [8]. In these experiments with constant pulse duration an amount of discharge energy is generated, this non productive heat is transferred to the work piece material that causes high temperature. When the discharge current is lower the discharge energy is also lower; the lower discharge energy results in low melting temperature, less evaporation and low impulsive force acting on machining region resulting in the formation of undulation recast layer. Therefore, the machined surface debris is expelled easily and rapidly from the machined zone. Some of the melted material adheres to the cathode and anode producing cracks and pores. The discharge current increases with the discharge energy increase. Higher discharge energy produces a higher melting temperature, increased evaporation and high impulsive forces acting on machined zone, that affects the higher uneven recast layer; micro cracks and pores are thus formed on the work piece surface.

The experimental results are depicted in variation of the recast layer thickness with span 20 surfactant concentration added in dielectric fluid as shown in Fig 7(B). When no surfactants were added to dielectric fluid, the recast layer thickness is extremely high. Further, the recast layer thickness reduces with the increase in the concentration of span 20 surfactant (4–6 g/lit), and the lower recast layer is obtained at the surfactant of 4 g/lit. When the surfactant concentration is higher than 6 g/lit the recast layer thickness increases. These experimental results supported the previous researcher's observation [17,18]. As mentioned earlier, when span 20 surfactant is mixed in dielectric fluid, it improves the viscosity, surface tension and dielectric strength. As the surfactant concentration increased, the overall dielectric concentration increases and some particles agglomerated on the machined surface.

The variation of graphite powder concentration on the recast layer thickness of the machined surface is as shown in Fig. 7(C). The experimental results presented show that the recast layer thickness is increased as graphite powder concentration increases. Further, when graphite powder concentration increases, there will be a slight decrease in the recast layer thickness. The reason may be due to graphite powder concentration effect on the machined surface which produces high discharge energy, high ignition spark and reduces the breakdown strength of the dielectric fluid [38,39]. When graphite powder is added to dielectric fluid, high pressure acts on the machined zone and causes an increase in the discharge channel gap and plasma channel [40]. Further, the molten material and powder particles are easily flushed; reducing the recast layer. When lower graphite powder concentration is added to dielectric fluid, the machined surface, recast layer thickness is not uniform and large undulation layers are formed. But, various cracks and pores are formed on the recast layer surface. Further, if high concentration of graphite powder is added in machining, the recast layer thickness may be uniform and small undulation layers are formed [41]. Another reason is as high concentration of graphite powder particles added into the dielectric and equally dispersion of the particles on the surface of the machining with constant pulse on time and pulse off time. This reduces the recast layer thickness.

Fig. 7 shows the $A_1B_1C_1$ parameters, i.e. discharge current of 10 Amp, surfactant concentration of 4 g/lit and graphite powder concentration of 4.5 g/lit respectively are the optimal conditions for RLT. Further the empirical model has been developed to predict the RLT values using regression analysis, including up to the square terms in the model. The regression equation is RLT = −41.7 + 2.64A + 10.7B + 1.91C − 0.0699A * A − 0.839B * B − 0.101C * C, R-Sq = 96.5 %, R2 and R2 adj values of the model are in the acceptable range of variability in predicting RLT values.

3.5. Confirmation test

As the optimum condition of EDM process parameters set is obtained, the conformation conditions are processed to check the performance parameters improvement. The results of confirmation test are compared with the outcome of the orthogonal array experimental values and prediction of the design operating parameter values. Table 14 shows the comparison of the experimental results using the initial (orthogonal array) and final (predict design) EDM process parameters on Titanium alloy.

3.6. Surface morphology

Fig. 8(A & B) shows the SEM micrographs of machined surface using surfactant 4 g/lit and powder concentration of 5 g/lit mixed with EDM process at a discharge current 10 A. The machined surfaces have shown irregular compound structures, droplets of debris, shallow craters and micro pores. The SEM micrograph shows the evidence of recast layer and micro cracks formed on the machined surface. The formation of surface cracks can be attributed to the variation of contraction stress within [42] the RLT and also surfactant and graphite powder effect on the dielectric fluid. More discharge energy is generated and more material is expelled resulting in frequent cracking. This gives rise to higher density of

Table 14
Validation of performance results.

Parameter	Optimum condition	Predicted optimum value	Experimental values
MRR (mm^3/min)	Discharge current (20 A) Surfactant (6 g/lit) Graphite powder (13.5 g/lit)	6.36	6.84
SR (μm)	Discharge current (10 A) Surfactant (4 g/lit) Graphite powder (4.5 g/lit)	1.90	1.95
EWR (mm^3/min)	Discharge current(10 A) Surfactant (8 g/lit) Graphite powder(13.5 g/lit)	0.38	0.35
RLT (μm)	Discharge current (10 A) Surfactant(4 g/lit) Graphite powder(4.5 g/lit)	13.86	13.30

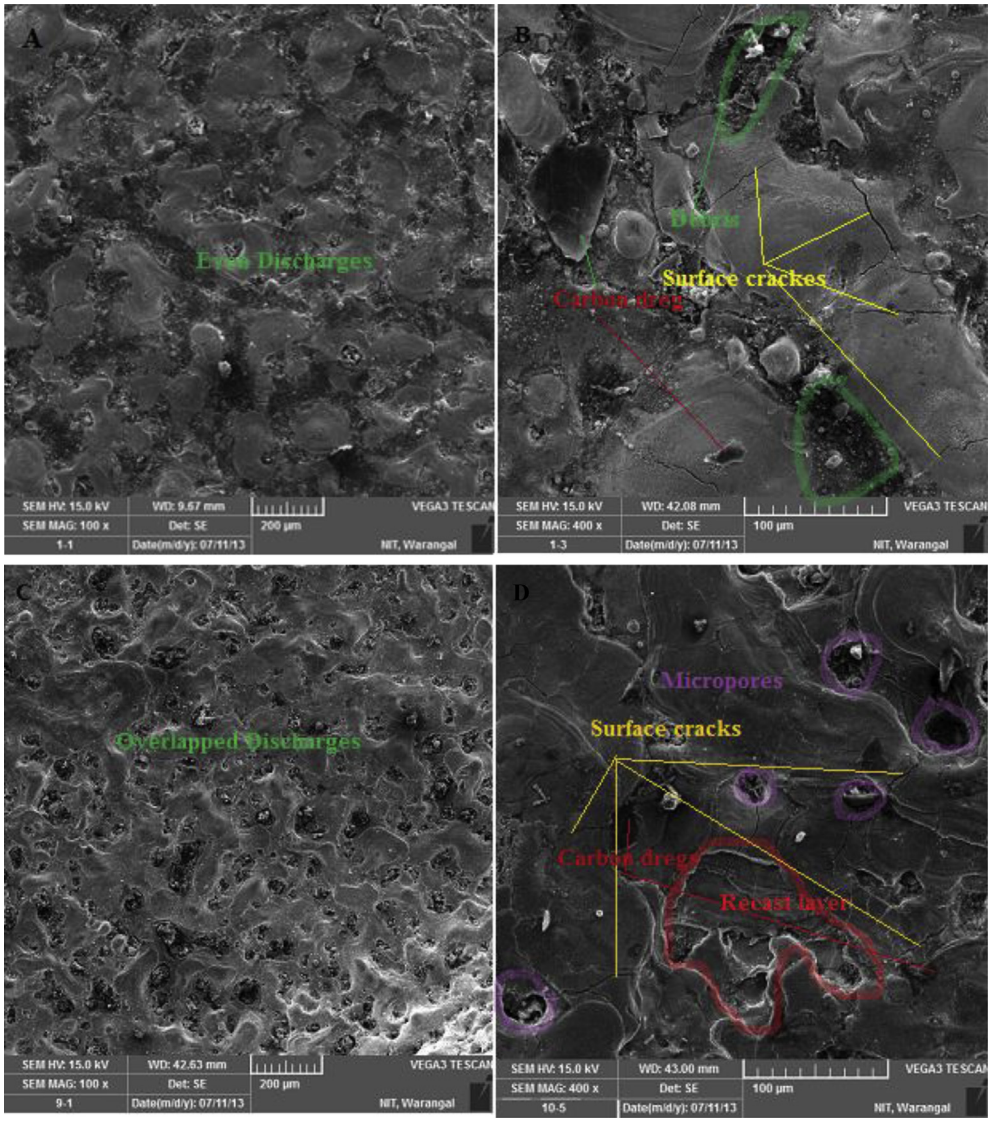

Fig. 8. A&B machined surface characteristics under discharge current of 10 A, Surfactant concentration 4 g/lit and graphite 4.5 g/lit. (At low surface roughness condition, (A) low magnification and (B) high magnification). C&D machined surface characteristics under discharge current of 20 A, Surfactant Concentration 6 g/lit and graphite 13.5 g/lit. (At high material removal rate condition, (C) low magnification and (D) high magnification).

globules accumulation at the close vicinity of machined zone which results in poorer surface finish.

Fig. 8(C & D) shows the SEM micrographs of machined surface at surfactant 6 g/lit and powder concentration of 13.5 g/lit mixed with EDM process at a discharge current 20 A. With increase in the discharge current, the surfactant concentration will increase the surface irregularities and this can be attributed to in the formation of deeper and larger craters. By increasing the discharge conditions

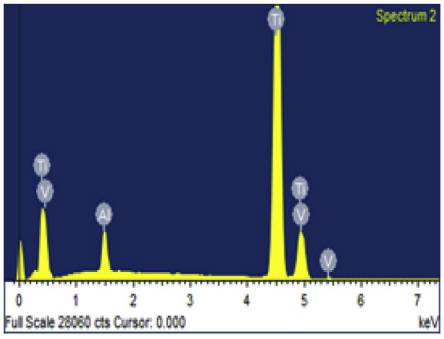

Element	Weight%	Atomic%
Al K	3.72	6.43
Ti K	94.28	91.74
V K	1.99	1.82
Totals	100.00	

Fig. 9. EDS Analysis of without machined titanium alloy.

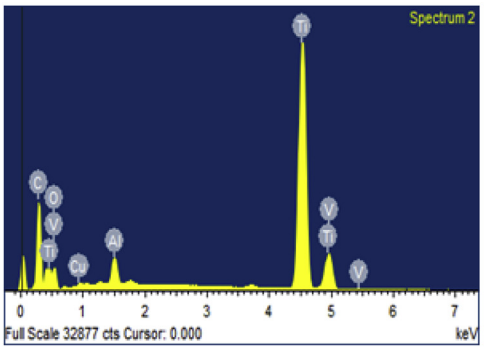

Element	Weight%	Atomic%
CK	28.70	55.86
OK	10.23	14.66
AK	1.01	.86
Ti K	58.64	28.06
V K	.71	.32
Cu L	0.61	0.24
Totals	100.00	

Fig. 10. EDS Analysis of with machined titanium alloy.

there is a large variation in the output degraded surfaces this can be due to increase in the discharge current, because of which a deep and large craters form.

3.7. EDS measurement

EDS analysis of work piece shows the presence of metal particles other than base metal. The metal particles moving from electrode to work piece are flushed out by continuous flow of dielectric fluid. Some amount of material is deposited on the machined surface of the work piece because of the particles that cannot be moved completely or flushed out of the discharge gap. This implies that a significant amount of material is transferred from the electrode to the work piece that is submerged in dielectric fluid. EDS results show improved quality and quantity values of elemental composition on the titanium work piece and copper electrode. Figs. 9 and 10 compares the EDS pattern of before and after machined samples, in order to investigate the chemical composition and to reveal the characteristics of the recast layer. When surfactant and graphite powder (concentration) is added into the EDM oil, there is an increase in the carbon content and during the machining process this carbon dissolves in the EDM oil and on the metal surface. In metal melting stage it forms TiC. Fig. 9 shows the existence of energy peak values on un-machined surface which was not found on the machined surface or on the recast layer. The EDS analysis reveals that the carbide, titanium and oxygen are major peaks which are present in Titanium metal surfaces.

Oxide formation is also noticed during EDS analysis of machined surface (Fig. 10). Oxidation occurs when oxygen attacks and degrades the EDM fluids. The process is accelerated by heat, light and metal catalysts in the presence of water, acids and solid contaminants. In this study, oxygen diffuses from the dielectric fluid into the melted metal and oxidizes the machined surface. By comparing the EDS results of the samples one may assume that other elements are formed on the recast layer in EDM oil.

4. Conclusions

The influence of surfactant and graphite powder mixed EDM of Ti-6Al-4V and also optimizing the process parameters such as discharge current, surfactant and powder concentrations using Taguchi method were performed and the following conclusions were drawn.

- The practical benefit of this study is that the use of obtained optimum condition improves the material removal rate, reduces surface roughness and less recast layer of Titanium alloy.
- Material removal rate at optimum condition (i.e. $A_3B_2C_3$) is increased with increase in the discharge current and graphite powder concentration. As the surfactant concentration increases from 4 to 6 g/lit, MRR increases, beyond 6 g/lit MRR decreases.
- The optimum condition for surface roughness was observed at $A_1B_1C_1$ having lower values of discharge current, surfactant and graphite powder concentration. It was observed that the SR is directly proportional to discharge current, surfactant and powder concentration.
- Tool wear rate at optimum condition (i.e. $A_1B_3C_3$) was lower at discharge current, higher at surfactant and graphite powder concentration. It was noticed that TWR is directly proportional to discharge current and inversely proportional to the surfactant and graphite powder concentration.
- Recast layer thickness at optimum condition (i.e. $A_1B_1C_1$) was lower at discharge current, surfactant and graphite concentration. It was observed the RLT is directly proportional to discharge current and powder concentration. As the Surfactant concentration increases RLT increases initially (4–6 g/lit), then decrease (6–8 g/lit).
- ANOVA and F-test of experimental data values related to the important process parameters of EDM revealed that discharge current (A) and surfactant concentration (C) influenced the MRR and TWR. Similarly, discharge current (A) and graphite powder concentration (B) affected on the SR and RLT.
- The SEM micrograph shows the evidence of recast layer and micro cracks formed on the machined surface. The formation of surface cracks on the machined surface is increasing the discharge energy with increase in the stresses reflected on it.

Acknowledgments

The authors would like to thank the authorities of National Institute of Technology-Warangal, Mishra Dhatu Nigam Ltd Hyderabad-India for providing the material.

References

[1] Valentin N. Moiseyev, Titanium Alloy: Russian Aircraft and Aerospace Applications, CRC press, 2006.
[2] Annie Ann Nee Liew, Optimization of Machining Parameters of Titanium Alloy in Electrical Discharge Machining Based on Artificial Neural Network, thesis, Dec 2010.
[3] K.P. Rajurkar, Gu Lin, Review of electrical discharge machining of titanium alloy, in: Proceedings of Seventh International Conference on Precision, Meso, Micro and Nano Engineering at COE, Pune, India, 2011, pp. 10–18.
[4] E.O. Ezugwu, Z.M. Wang, Titanium alloys and their machinability – a review, J. Mater. Process. Technol. 68 (1997) 262–274.
[5] C.H.C. Haron, A. Jawaid, The effect of machining on surface integrity of titanium alloy Ti–6Al–4V, J. Mater. Process. Technol. 166 (2005) 188–192.
[6] D.A. Dornfeld, J.S. Kim, H. Dechow, J. Hewsow, L.J. Chen, Drilling burr formation in titanium alloy Ti–6Al–4V, Ann. CIRP 48 (1999) 73–76.
[7] Takashi Endo, Takayuki Tsujimoto, Kimiyuki Mitsui, The effect of vibration on machining time and stability of discharge processing 32 (2008) 269–277.

[8] Chow Han-Ming, Yang Lieh-Dai, Lin Ching-Tein, Chen Yuan-Feng, The use of SiC powder in water as dielectric for micro-slit EDM machining, J. Mater. Process. Technol. 195 (2008) 160–170.
[9] G. Kenneth, J.R. Heinz, Fundamental Study of Magnetic Field-assisted Micro-EDM for Non-magnetic Materials, thesis, 2010.
[10] N.J. Churi, Z.C. Li, Z.J. Pei, C. Treadwell, Rotary Ultrasonic Machining of Titanium Alloy, 2005, pp. 885–892. IMECE-80254.
[11] P. Govindan, R. Agarwal, S.S. Joshi, Experimental Investigation on Dry EDM Using Helium Gas Dielectric, AIMTDR, Visakhapatnam, India, 2010.
[12] S. Abdulkareem, A. Khan, M. Konneh, Reducing electrode wear ratio using cryogenic cooling during electrical discharge machining, Int. J. Adv. Manuf. Technol. 45 (2009) 1146–1151.
[13] M.L. Jeswani, Effect of the addition of graphite powder to kerosene used as the dielectric fluid in electrical discharge machining, Wear 70 (2) (1981) 133–139.
[14] G. Kibria, B. Sarkar, B.R. Pradhan, B. Bhattacharyya, Comparative study of different dielectrics for micro-EDM performance during microhole machining of Ti–6Al–4V alloy, Int. J. Adv. Manuf. Technol. 48 (5–8) (2009) 557–570.
[15] K. Murahari, A. Kumar, Influence of span20 surfactant and graphite powder added in dielectric fluid on EDM of titanium alloy, J. Ind. Eng. Manag. Sci. 4 (2014) 62–67.
[16] K. Murahari, A. Kumar, Effect of additives added in dielectric fluid on electrical discharge machining of titanium alloy, in: Proceedings of the ICARMMIEM, 2014, pp. 52–59. India.
[17] K.L. Wu, B.H. Yan, J.W. Lee, C.G. Ding, Study on the characteristics of electrical discharge machining using dielectric with surfactant, J. Mater. Process. Technol. 209 (2009) 3783–3789.
[18] K.L. Wu, B.H. Yan, F.Y. Huang, Chen, Improvement of surface finish on SKD steel using electro-discharge machining with aluminum and surfactant added dielectric, Int. J. Mach. Tools Manuf. 45 (2005) 1195–1201.
[19] A.S. Dukhin, P.J. Goetz, Ionic Properties of So-called Non-ionic Surfactants in Non-polar Liquids, Dispersion Technology, Inc., New York, 2004, pp. 1–21.
[20] Yanzhen Zhang, Youghong Liu, Renie Ji, Sinking EDM in water in oil emulsion, Int. J. Adv. Manuf. Technol. (2012).
[21] Youghong Liu, Renie Ji, Yanzhen Zhang, Haifeng Zhang, Investigation of emulsion for die sinking EDM, Int. J. Adv. Manuf. Technol. 47 (2010) 403–409.
[22] W. Konig, L. Jorres, Aqueous solution of organic compounds as dielectric for EDM sinking, Ann. CIRP 36 (1) (1987).
[23] A.M. Nikalje, Raj Deep Gupta, A. Kumar, Analysis of recast layer and surface machined by electrical discharge machining, in: International Conference on Recent Advances in Mechanical Engineering, Dr. M.G.R. Educational and Research Institute University, Chennai, 19–20, April, 2012.
[24] Y. Zhang, Y. Liu, R. Ji, B. Cai, H. Li, Influence of dielectric type on porosity formation on electrical discharge machined surfaces, Metall. Mater. Trans. B 43 (4) (2012) 946–953.
[25] P.J. Ross, Taguchi Techniques for Quality Engineering, Mc Graw-Hill, New York, 1998, pp. 24–98.
[26] D.C. Montgomery, Design and Analysis of Experiments, Wiley, New York, 1997, pp. 395–476.
[27] S. Phadke Madhav, Quality Engineering Using Robust Design, Prentice Hall, Englewood Cliffs, New Jersey, 1989, pp. 41–229.
[28] Norliana Mohd Abbas, Darius G. Solomon, Md. Fuad Bahari, A review on current research trends in electrical discharge machining (EDM), Int. J. Mach. Tools Manuf. 47 (2007) 1214–1228.
[29] J.Q. Feng, D.A. Hays, Relative importance of electrostatic forces on powder particles, Powder Technol. 135 (2003) 65–75.
[30] T. Masuzawa, K. Tanaka, Water based dielectric solution for EDM, Ann. CIRP 32/1 (1983).
[31] H.K. Kansal, Sehijpal Singh, Technology and research developments in powder mixed electric discharge machining (PMEDM), J. Mater. Process. Technol. 184 (2007) 32–41.
[32] B.H. Yan, Y.C. Lin, F.Y. Hung, C.H. Wang, Surface modification of SKD61 during EDM with metal powder in dialectric, Mater. Trans. 42 (12) (2001) 2597–2604.
[33] W.S. Zhao, Q.G. Meng, Z.L. Wang, The application of research on powder mixed EDM in rough machining, J. Mater. Process. Technol. 129 (2002) 130–138.
[34] M.J. Rosen, Surfactants and Interfacial Phenomena, third ed., Wiley Interscience, New York, 2004, pp. 311–324.
[35] D.J. Shaw, Introduction to Colloid and Surface Chemistry, fourth ed., Butterworth–Heinemann, Oxford, 1992, pp. 76–90.
[36] A. Erden, Kaftanoğlu B, Thermo-mathematical modelling and optimization of energy pulse forms in electrical discharge machining, in: IJMTDR, vol. 21(1), 1981, pp. 11–22.
[37] W. Rehbein, H.P. Schulze, K. Mecke, G. Wollenberg, M. Storr, Influence of selected groups of additives on breakdown in EDM sinking, J. Mater. Process. Technol. 149 (1) (2004) 58–64.
[38] Syed Khalid Hussain, Kuppan Palaniyandi, Performance of electrical discharge machining using aluminium powder suspended distilled water, Turk. J. Eng. Environ. Sci. 36 (3) (2012) 195–207.
[39] Y.S. Wong, L.C. Lim, I. Rahuman, W.M. Tee, Near-mirror-finish phenomenon in EDM using powder-mixed dielectric, J. Mater. Process. Technol. 79 (1998) 30–40.
[40] W.S. Zhao, Q.G. Meng, Z.L. Wang, The application of research on powder mixed EDM in rough machining, J. Mater. Process. Technol. 129 (1) (2002) 30–33.
[41] A. Okada, Y. Uno, K. Hirao, T. Takagi, Formation of hard layer by EDM with carbon powder mixed fluid using titanium electrode, in: Proceedings of 5th International Conference on Progress of Machining Technology, ICPMT, USA, 2000, pp. 464–469.
[42] L.C. Lee, L.C. Lim, V. Narayanan, V.C. Venkatesh, Quantification of surface damage of tool steels after EDM, Int. J. Mach. Tools Manuf. 28 (4) (1988) 359–372.